Supporting Information

DFT-assisted ^{31}P and ^{23}Na MAS-NMR study of the $Na_3V_2(PO_4)_2F_3$ – $Na_3V_2(PO_4)_2FO_2$ solid solution: unravelling its local and electronic structures

*Long H. B. Nguyen [a,b,c], Paula Sanz Camacho [a,c], Thibault Broux [a,b,c,d], Jacob Olchowka [a,c,d], Christian Masquelier [b,c,d], Laurence Croguennec [a,c,d], and Dany Carlier [a,c,d] **

[a] CNRS, Univ. Bordeaux, Bordeaux INP, ICMCB UMR CNRS #5026, F-33600, Pessac, France.

[b] Laboratoire de Réactivité et de Chimie des Solides, Université de Picardie Jules Verne, UMR CNRS #7314, 80039 Amiens Cedex 1, France.

[c] RS2E, Réseau Français sur le Stockage Electrochimique de l'Energie, FR CNRS #3459, F-80039 Amiens Cedex 1, France.

[d] ALISTORE-ERI European Research Institute, FR CNRS #3104, Amiens, F-80039 Cedex 1, France.

Corresponding author: D. Carlier (Email: Dany.Carlier@icmcb.cnrs.fr)

Figure S1: (*Left*) Experimental structure of $Na_3V_2(PO_4)_2F_3$ determined by synchrotron X-ray powder diffraction [30], and (*Right*) Input model used for DFT calculations where a fully occupied Na site represents the partial occupied Na2 and Na3 sites in the actual structure.

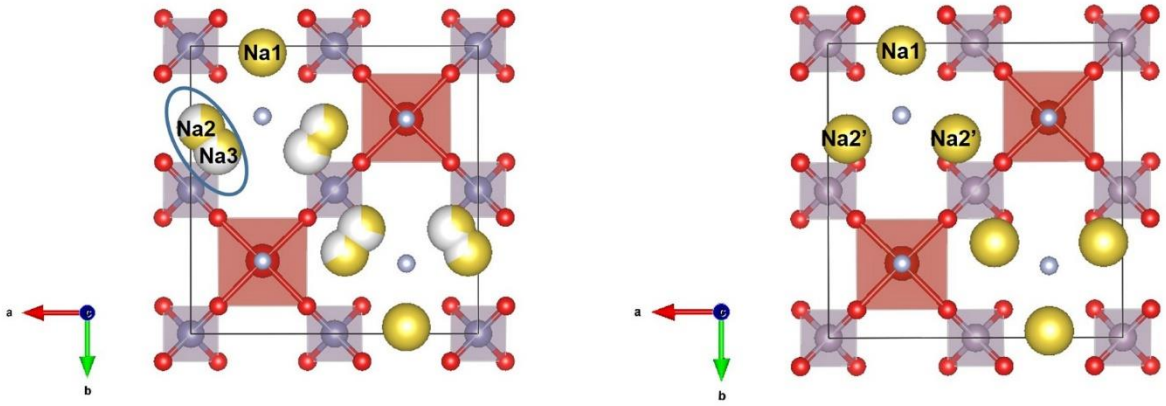

Table S1: Calculated unit cell parameters of $Na_3V_2(PO_4)_2F_3$ after geometry optimization using GGA and GGA+U methods compared to the experimental ones.

	Synchrotron X-ray powder diffraction	**GGA**	**GGA + 3eV**	**GGA + 4eV**	**GGA + 5eV**
***a* (Å)**	9.02847(3)	9.096	9.126	9.150	9.178
***b* (Å)**	9.04444(3)	9.156	9.193	9.215	9.235
***c* (Å)**	10.74666(6)	10.758	10.890	10.895	10.902
α	90º	90º	90º	90º	90º
β	90º	90º	90º	90º	90º
γ	90º	90º	90º	90º	90º

Figure S2: (*Left*) Experimental structure of $Na_3V_2(PO_4)_2FO_2$ determined by single crystal diffraction,[15] and (*Right*) Input model used for DFT calculations where a fully occupied Na3' site represents the half occupied Na2 sites in the actual structure.

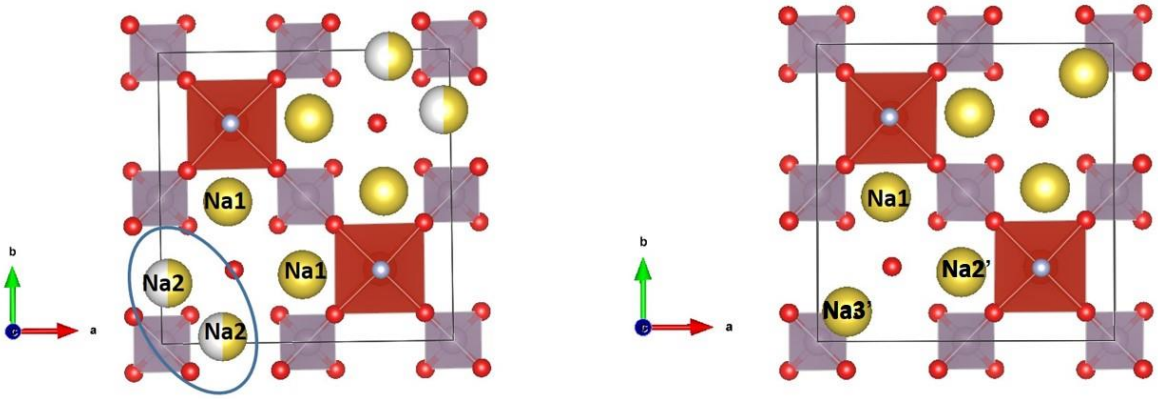

Table S2: Calculated unit cell parameters of $Na_3V_2(PO_4)_2FO_2$ after geometry optimization using GGA and GGA+U methods compared to the experimental ones.

	Synchrotron X-ray powder diffraction	**GGA**	**GGA + 3eV**	**GGA + 4eV**	**GGA + 5eV**
***a* (Å)**	9.0285(1)	9.092	9.138	9.152	9.167
***b* (Å)**	9.0285(1)	9.092	9.138	9.152	9.167
***c* (Å)**	10.6149(2)	10.624	10.591	10.587	10.569
α	90°	90°	90°	90°	90°
β	90°	90°	90°	90°	90°
γ	90°	90°	90°	90°	90°

Figure S3: The degeneracy of five 3*d* orbitals under vacuum and the splitting scheme of these orbitals in $Na_3V^{3+}{}_2(PO_4)_2F_3$ and in $Na_3(V^{4+}O)_2(PO_4)_2F$.

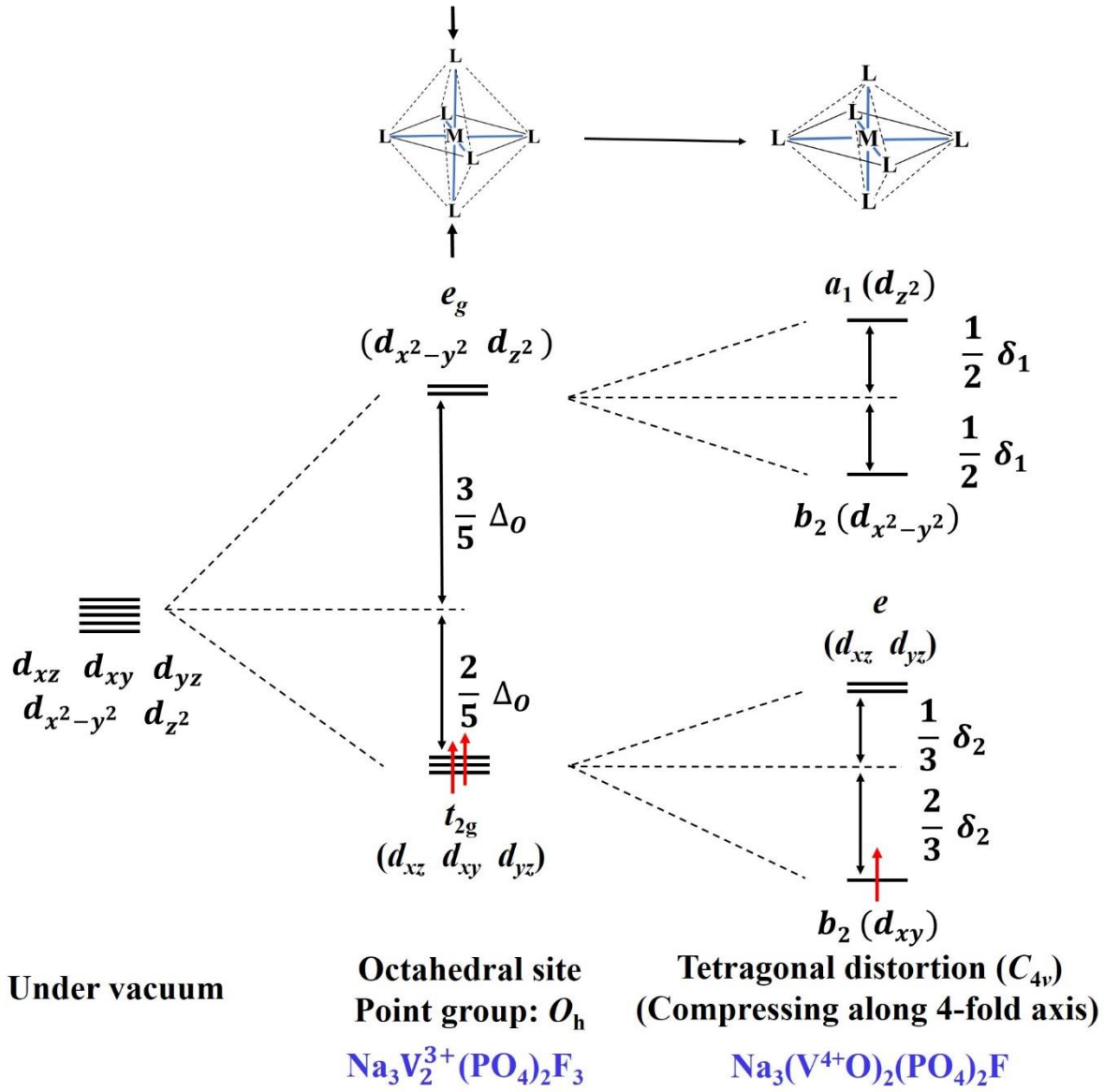

Figure S4: Different ways to distribute V^{3+} and V^{4+} in $Na_3V_2(PO_4)_2F_2O$ (y' = 1.0) structure. $V^{3+}O_4F_2$ and $V^{4+}O_5F_1$ units are depicted as red and blue octahedra, respectively. The corresponding formation energies of each configuration are given below the models.

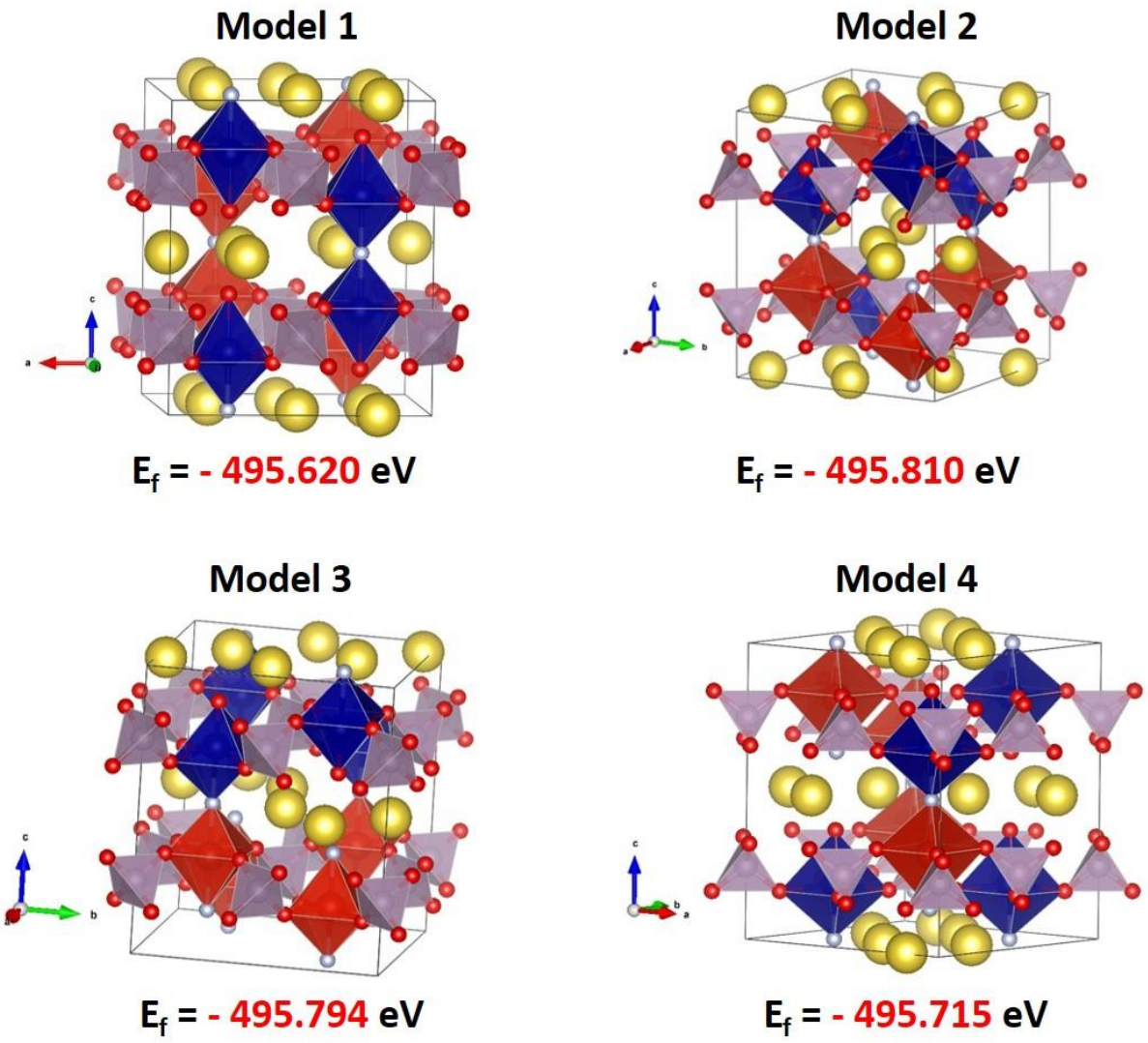

Figure S5: (*a* and *b*) The spin distribution map showing $P(OV^{3+})_3(OV^{4+})$ and $P(OV^{3+})(OV^{4+})_3$ local environments in Model 2 of $Na_3V_2(PO_4)_2F_2O$; (*c* and *d*) The spin distribution map showing $P(OV^{3+})_4$ and $P(OV^{4+})_4$ local environments in Model 3 of $Na_3V_2(PO_4)_2F_2O$.

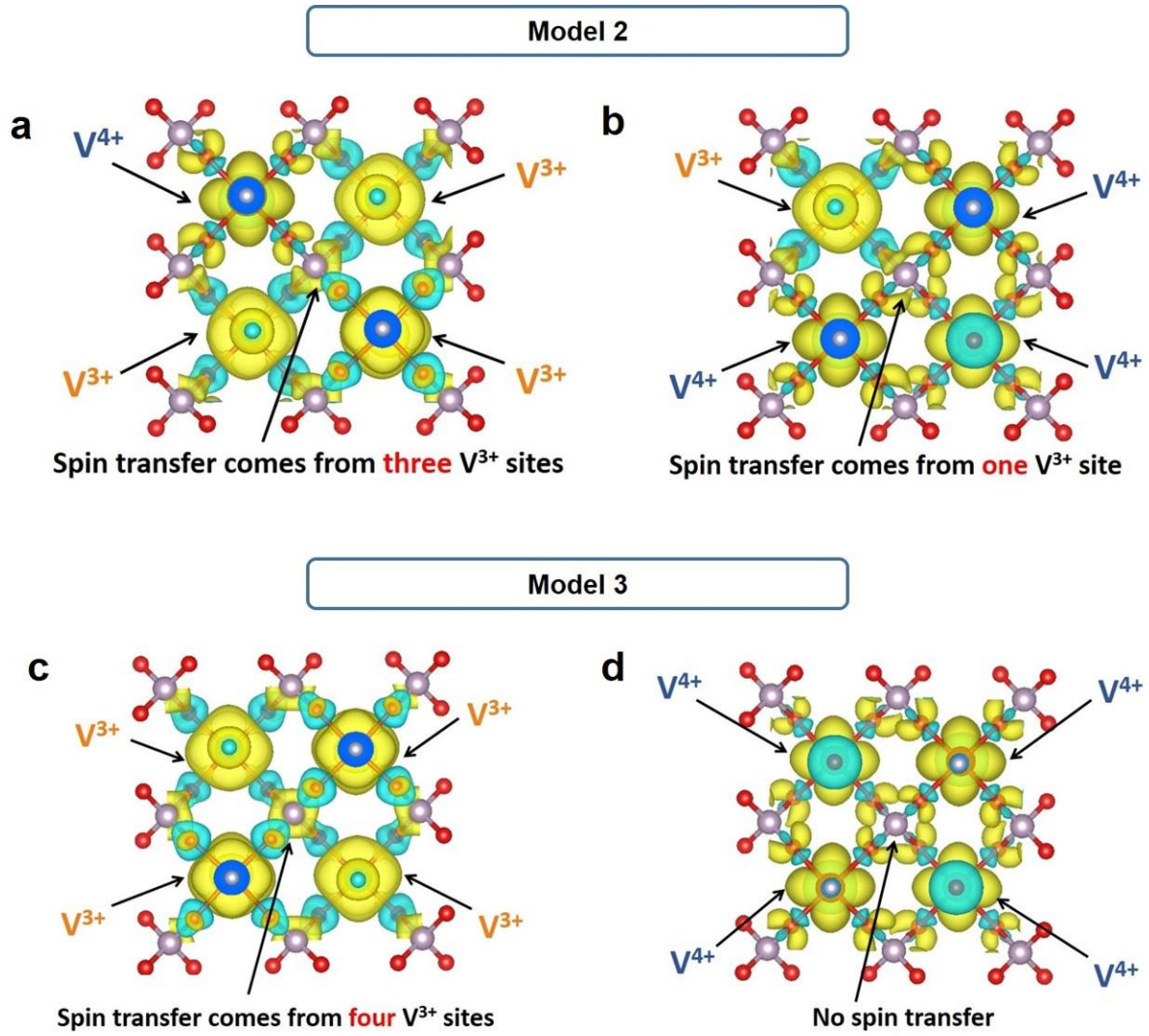

Figure S6: Local environments of different Na sites in $Na_3V_2(PO_4)_2F_3$ material. Oxygen atoms are depicted in red and fluorine atoms are depicted in light grey.

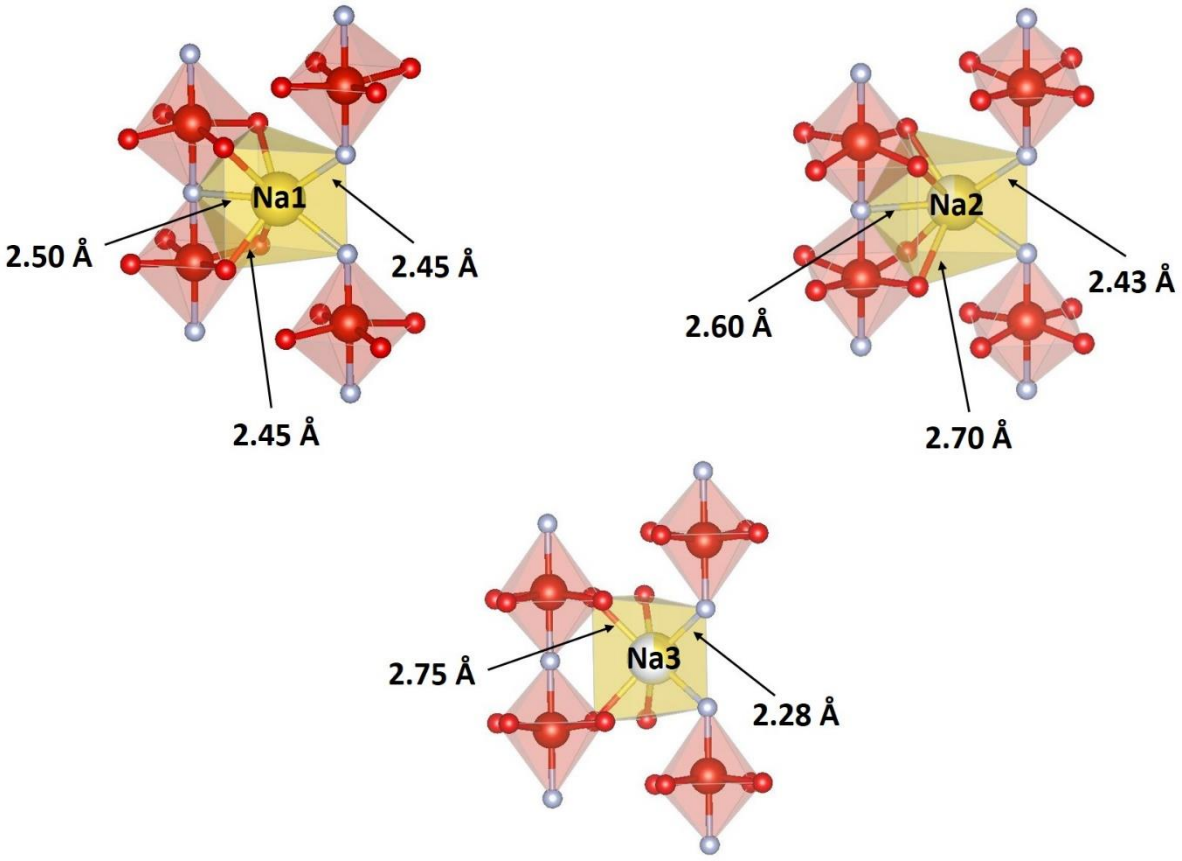

Table S3: The ^{23}Na *ss*-NMR chemical shifts (in ppm) calculated by GGA and GGA+U methods for sodium nuclei in $Na_3V_2(PO_4)_2F_3$ and $Na_3V_2(PO_4)_2FO_2$ structures.

$Na_3V_2(PO_4)_2F_3$					
	Experimental data	**GGA**	**GGA+3*eV***	**GGA+4*eV***	**GGA+5*eV***
Na1 (x4)	~ 139.6 ppm	270 – 273 ppm	166 ppm	152 ppm	131 ppm
Na2 (x8)		205 – 258 ppm	133 ppm	118 ppm	102 ppm
$Na_3V_2(PO_4)_2FO_2$					
Na1 (x4)	~ 80 ppm	77 ppm	6 ppm	-31 ppm	-65 ppm
Na2 (x8)		94 ppm	59 ppm	32 ppm	2 ppm

Table S4: The ^{23}Na *ss*-NMR chemical shifts (in ppm) of sodium nuclei in $Na_3V_2(PO_4)_2F_2O$, considering different structural models and calculated by GGA method.

	Model 1	**Model 2**	**Model 3**	**Model4**
Na1	187	243	125	185
Na2	152	82	187	185
Na3	200	33	172	167
Na4	95	90	88	167
Na5	152	58	165	185
Na6	187	153	125	185
Na7	95	288	175	167
Na8	200	116	181	167
Na9	100	30	179	166
Na10	200	107	180	166
Na11	200	82	191	166
Na12	100	116	90	166

Figure S7: The evolution of the relative intensity between different ^{31}P *ss*-NMR resonances in $Na_3V_2(PO_4)_2F_2O$ as the function of the off-set positions (800 ppm, 2978 ppm, and 5000 ppm).

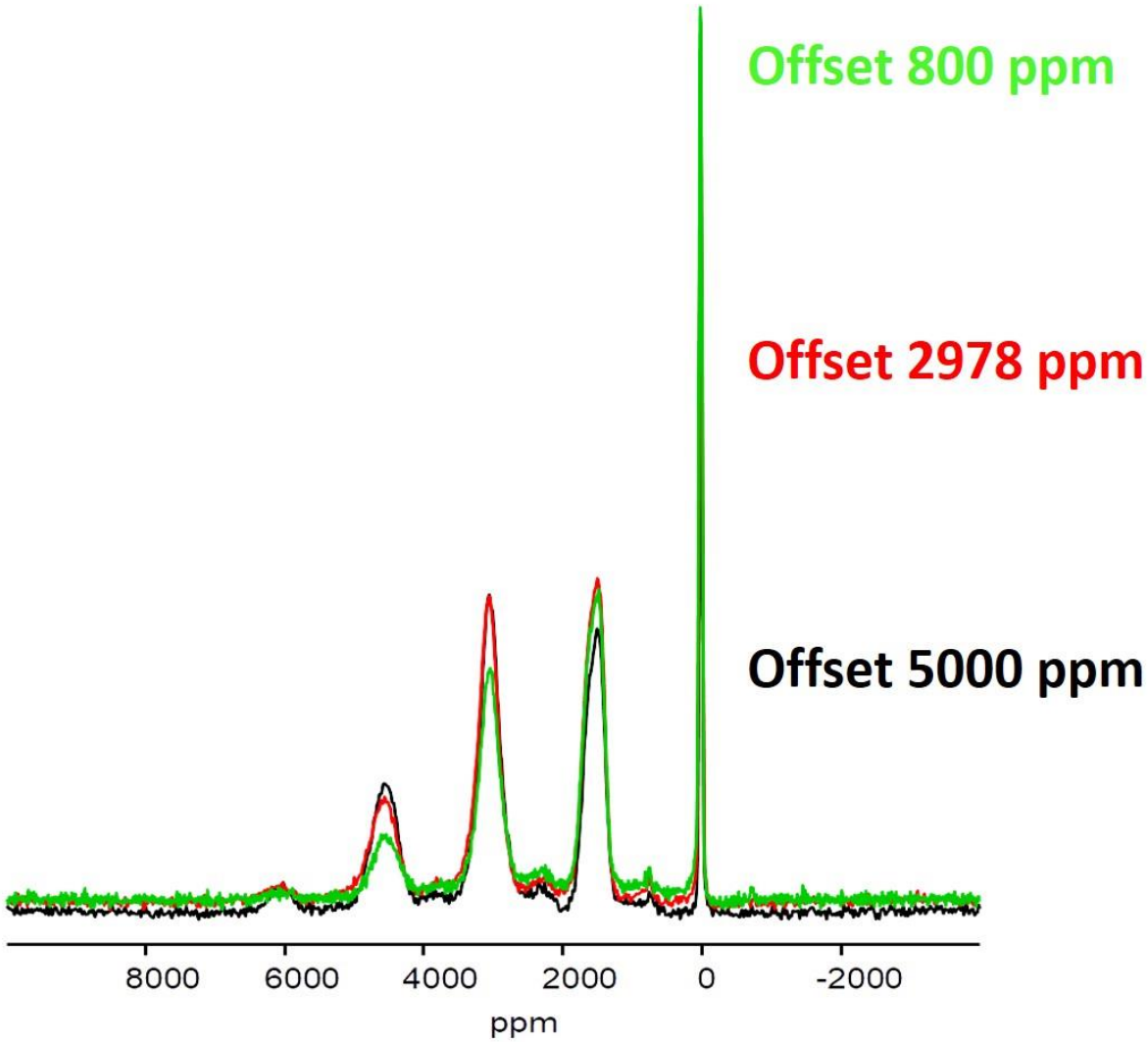

^{31}P ss-NMR spectra were acquired on a Bruker Avance III 100 MHz spectrometer, equipped with a 2.4 T widebore magnet (operating at Larmor frequency of 40.6 MHz for ^{31}P) by using a standard Bruker 2.5 mm MAS probe at 30 kHz MAS rate. Chemical shifts are referenced relative to an aqueous H_3PO_4 85% (Sigma-Aldrich) solution at 0 ppm. In each case, a Hahn echo sequence was used with a $\pi/2$ pulse of 1.0 μs and a recycle delay of 0.2 s. The position of the offset (800, 2978 and 5000 ppm) had been changed to see any effect on the relative intensities of each resonance.

Figure S8: The change in the relative intensity between different ^{31}P *ss*-NMR resonances in $Na_3V_2(PO_4)_2F_2O$ at different refocalization delays.

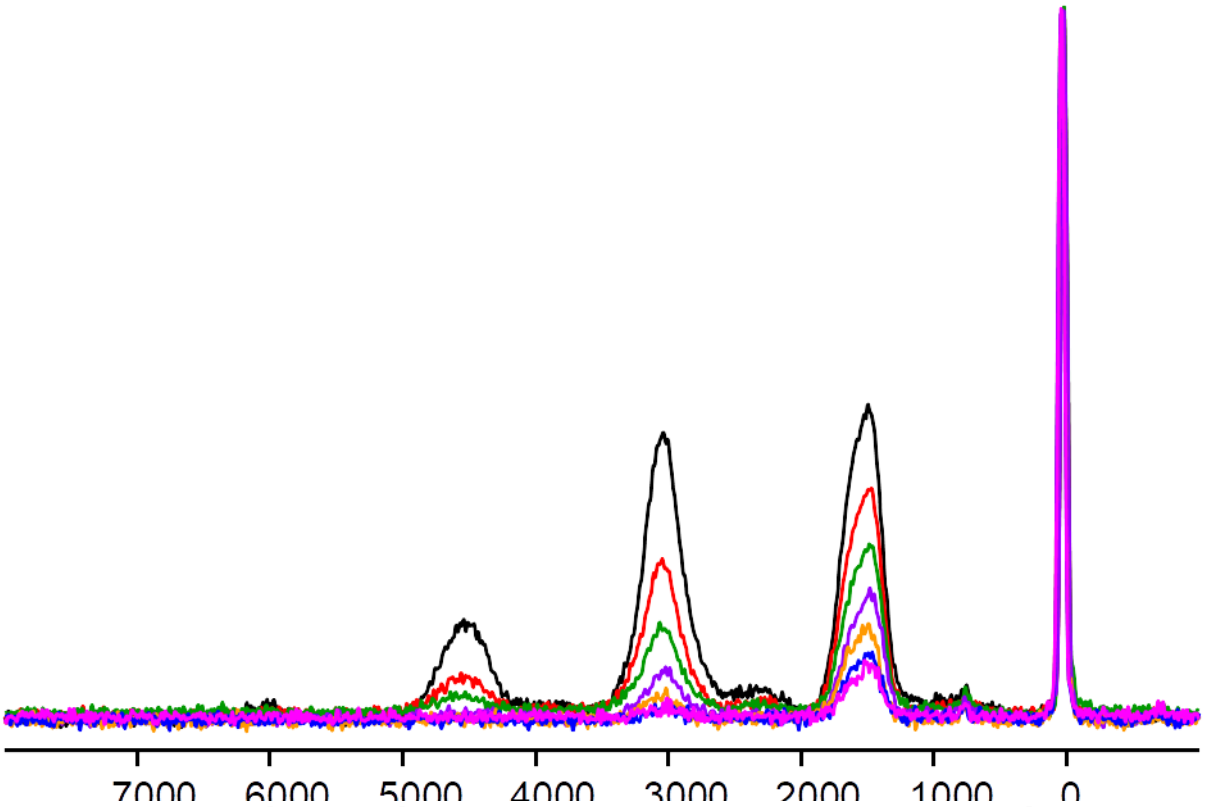

^{31}P ss-NMR spectra were acquired on a Bruker Avance III 100 MHz spectrometer, equipped with a 2.4 T widebore magnet (operating at Larmor frequency of 40.6 MHz for ^{31}P) by using a standard Bruker 2.5 mm MAS probe at 30 kHz MAS rate. Chemical shifts are referenced relative to an aqueous H_3PO_4 85% (Sigma-Aldrich) solution at 0 ppm. In each case, a Hahn echo sequence was used with a $\pi/2$ pulse of 1.0 µs and a recycle delay of 0.2 s where the d6 was changed from 1s (black spectrum) to 7s (pink spectrum) progressively.

Table S5: A comparison of the experimental and theoretical relative intensities between the three main ^{23}Na *ss*-NMR resonances observed for the $Na_3V_2(PO_4)_2F_3$ – $Na_3(VO)_2(PO_4)_2F$ solid-solution.

	Calculated			**Observed**		
	$Na(OV^{3+})_2$	**$Na(OV^{3+})(OV^{4+})$**	**$Na(OV^{4+})_2$**	**$Na(OV^{3+})_2$**	**$Na(OV^{3+})(OV^{4+})$**	**$Na(OV^{4+})_2$**
$Na_3V_2(PO_4)_2F_3$	100%			95%	5%	
$Na_3V_2(PO_4)_2F_{2.8}O_{0.2}$	81%	18%	1%	81%	19%	
$Na_3V_2(PO_4)_2F_{2.6}O_{0.4}$	64%	32%	4%	53%	40%	7%
$Na_3V_2(PO_4)_2F_{2.4}O_{0.6}$	49%	42%	9%	47%	45%	8%
$Na_3V_2(PO_4)_2F_{2.2}O_{0.8}$	36%	48%	16%	39%	49%	11%
$Na_3V_2(PO_4)_2F_2O$	25%	50%	25%	31%	53%	16%
$Na_3V_2(PO_4)_2F_{1.5}O_{1.5}$	6.25%	37.5%	56.25%	7%	24%	69%
$Na_3V_2(PO_4)_2FO_2$			100%		3%	97%